A comparative study of Fe-Cr unmixing using differential scanning calorimetry and small-angle scattering

Laurent Couturier, Frédéric de Geuser, Alexis Deschamps

A comparative study of Fe-Cr unmixing using differential scanning calorimetry and small-angle scattering

Laurent Couturier[1,2], Frédéric De Geuser[1], Alexis Deschamps[1]

[1] Univ. Grenoble Alpes, CNRS, Grenoble INP, SIMAP, 38000 Grenoble, France

[2] Université de Nantes, CNRS, Institut des Matériaux Jean Rouxel, IMN, F-44000 Nantes, France

Corresponding author :

laurent.couturier@uninv-nantes.fr

Institut des Matériaux Jean Rouxel (IMN), Rue Christian Pauc, BP50609, 44306 Nantes Cedex3

Keywords

Fe-Cr unmixing, stainless steel, small-angle scattering (SAS), differential scanning calorimetry (DSC), spinodal decomposition

Highlights

- Stainless steel Fe-Cr unmixing can be characterized using modulated DSC during solutionizing heat treatment of aged material
- Transformation's enthalpy and temperature show significant evolution even for very early decomposition stages
- Transformation's enthalpy and temperature are respectively correlated to composition fluctuations' amplitude and correlation length measured using small-angle scattering

Color should not be used for any figures in print.

Abstract

Fe-Cr unmixing in stainless steels is an issue of great importance in industry restricting the use of these materials at middle range temperatures (around 300°C – 500°C). The study of this phenomenon is difficult due to its very small scale (a few tenth to a few nanometers) and the fact that Fe and Cr have very similar crystallographic structures and atomic number. This imposes the use of very advanced (and expensive) characterization techniques requiring a strong expertise such as Atom Probe Tomography (APT) or Small Angle Scattering (SAS) of neutrons or X-rays. In contrast, this work shows that Fe-Cr unmixing can be characterized with high sensitivity using Differential Scanning Calorimetry (DSC). A methodology to measure the enthalpy and peak temperature of the reversion of the Cr composition fluctuations above the miscibility gap is presented. These characteristics measured on aged 15-5 PH stainless steel samples over a wide range of temperatures and times are compared with SAXS characterization of the Cr unmixing. Finally, phenomenological relationships are deduced between the enthalpy and peak temperature from DSC and amplitude and characteristic length of Cr composition fluctuations from SAXS.

1. Introduction

The unmixing of Fe-Cr solid solution is a concern in many industrial applications (nuclear power plants, aeronautics…) where stainless steels – ferritic, martensitic and duplex – are employed at medium temperatures – typically in-between 300°C and 500°C, depending on the alloy composition – limiting the exposition time in this temperature range and/or restraining the use of these alloys below 300°C [1–5]. This very slow decomposition of the BCC phase, due to the presence of a miscibility gap in the Fe-Cr binary system, is causing continuous embrittlement of the alloy which is also known as the 475°C (885°F) embrittlement of ferritic stainless steels [1,3,4]. Due to its very large impact on the industrial use of stainless steels, this Fe-Cr decomposition has been extensively studied over the past decades. Experimental characterization of the degree of unmixing has been mainly carried out using Atom Probe Tomography (APT) [2,4,6–15] and Small-Angle Scattering (using neutrons or X-rays, respectively SANS and SAXS) [16–25]. These experimental data have extensively served as a basis for establishing the validity of physically-based models, most often using Kinetic Monte Carlo modelling, and for establishing the link between the degree of unmixing and the evolution of mechanical properties [2,4,9,15,24,26–30].

Both APT and SAS aim at characterizing the spatial fluctuations of the concentration in Cr. Results provide characteristic dimensions of these fluctuations and their amplitude, as well as auto-correlation (or radial distribution) functions. It has been recently demonstrated that a common framework could be used to derive such parameters from the two types of measurements [31]. However, these experimental techniques suffer from some drawbacks.

APT measurements provide very local information, which may be difficult to generalize in case of a material containing inhomogeneity at the scale of an APT tip or larger – $\gtrsim$ 100 nm. This is often the case in complex stainless steels, which may contain both austenite and ferrite, and a complex distribution of substitutional species in addition to Cr. Additionally, realizing APT measurements is time-consuming and intrinsic limitations exist to detect composition fluctuations of very small dimensions (sub-nanometric) [32].

Small-Angle Scattering, on the other hand, is well suited to measure a large number of samples or to realize in-situ measurements. However, Fe-Cr composition fluctuations are of small magnitude, especially during early stages of unmixing, and the contrast in electron density between Fe and Cr is small, so that the measured signals are generally weak and require the use of large scale facilities, neutron sources or synchrotron X-ray sources, with little availability for systematic routine measurements. Thus, there is a strong need for a versatile, easily accessible measurement method, for assessing the degree of unmixing of the Fe-Cr solid solution in stainless steels.

As any phase transformation, Fe-Cr unmixing results in enthalpy changes that can be measured by calorimetry methods. While the isothermal unmixing kinetics is so slow that enthalpy changes cannot be measured in situ, this is not the case of the reversion of a phase separated microstructure being heated back to a homogeneous solid solution, since this reversion will take place at a temperature higher than that of the unmixing, where the atomic mobility is larger. Differential Scanning Calorimetry (DSC) or Differential Thermal Analysis (DTA) has been occasionally used to assess the degree of phase separation in Fe-Cr based alloys [33,34]. Being a bulk technique, with easy data analysis, such experiments are promising candidates for establishing a routine analysis tool overcoming most of the drawbacks presented above. However, there is no direct way to link the data from a DSC thermogram to the characteristics of unmixing (characteristic length and amplitude of composition fluctuations).

The present work aims at establishing such links, for the special case of the long-term aging of a precipitation hardening stainless steel 15-5PH, by performing a systematic comparison between DSC experiments and SAXS measurements, realized in anomalous mode at the Cr edge with a synchrotron source to maximize the contrast and thus the data quality. This comparison will be carried out over a wide range of aging times and temperatures, so that very early and relatively late stages of aging, with different combinations of dimension and amplitude, will be available to assess the robustness of the comparison.

2. Experimental procedure

The present study was carried out on a 15-5PH stainless steel whose nominal composition is given in **Table 1**. Prior to long-term ageing, the material was subjected to a solutionizing treatment of about 80 min at 1000°C followed by an air quench and a precipitation hardening treatment of 5 h at 505°C performed by the material's supplier, Aubert & Duval. The initial microstructure consists of a martensitic matrix containing Cu precipitates with an average size of 2.6nm and a volume fraction of about 3%, and a small fraction of austenite. More details of the initial microstructure and its evolution during long term ageing can be found in our previous publication [35].

Long-term aging of this material was carried out at six different temperatures ranging from 290°C to 420°C for various durations up to 15,000 h for the lowest aging temperatures.

	Cr	Ni	Cu	Mn	Si	Mo	Nb	C	P	S	Fe
%wt	14.87	4.93	2.99	0.8	0.38	0.27	0.21	0.025	0.019	<0.002	bal.
%at	15.85	4.65	2.61	0.81	0.75	0.16	0.13	0.115	0.034	<0.004	bal.

Table 1: Nominal chemical composition of the studied stainless steel.

For each aging condition (temperature and duration), the samples used for DSC and SAXS experiments in this work originate from the same piece of aged material and all aged pieces originate from a single material beam.

SAXS samples were cut from the various aged material blocks in the shape of 0.3 mm thin sheets which were then ground down to about 40 µm ± 20 µm using mechanical polishing. SAXS experiments were conducted at the D2AM beamline (BM02) of the European Synchrotron Radiation Facility (ESRF) using X-Ray energy just below the Cr absorption edge (5.983 keV) to benefit from the anomalous effect (contrast increase) for the Fe-Cr unmixing measurements. The detector was a 2D-CCD camera, whose images were corrected for electronic noise, spatial distortion, pixel efficiency and background noise. The measured intensity was normalized using the measurements of the transmission of each specimen and of a glassy carbon reference sample [36]. An azimuthal averaging has been computed from all corrected images since the measured scattered intensity for all aging condition is isotropic over a scattering vector range of [$3x10^{-2}$ $Å^{-1}$, $6x10^{-1}$ $Å^{-1}$]. The advancement of unmixing was characterized by 2 parameters: the amplitude of the composition fluctuations and their correlation length. They were extracted from the SAXS data using a model established in a previous work [31]. A detailed presentation of the SAXS data as a function of aging conditions can be found in [24].

DSC samples were cut from the same aged material blocks in shape of approximately 3.5 x 3.5 x 0.8 mm^3 parallelepipeds. All DSC measurements were performed under high purity nitrogen flow. A TA Q200 DSC instrument was used, allowing to cover a scanning range of 200°C to 550°C and the use of modulated heating and cooling ramps. The scanning rate was 5°C.min^{-1} and the amplitude and period of the temperature's modulation were respectively 2°C and 2 min. The modulation of the temperature during scanning presents two advantages. The first one is the ability to separate the reversing and non-reversing contributions to the heat flux variation. The former is mainly due to the heat capacity of the material and the latter is due to the phase transformations occurring within the material [37]. In our case, only the non-reversing heat flux was of interest since we are looking for the quantification of the solutionizing of chromium and iron composition fluctuations due to aging. The second interest of the temperature modulation is a higher instantaneous temperature scanning rate which gives rise to a stronger measured signal [38,39] – being of particular importance for the very early stages of decomposition, where the signal is expected to be very low.

The whole thermal history of the material is schematically summarised in **Figure 1**, from its elaboration until the end of the DSC experiment.

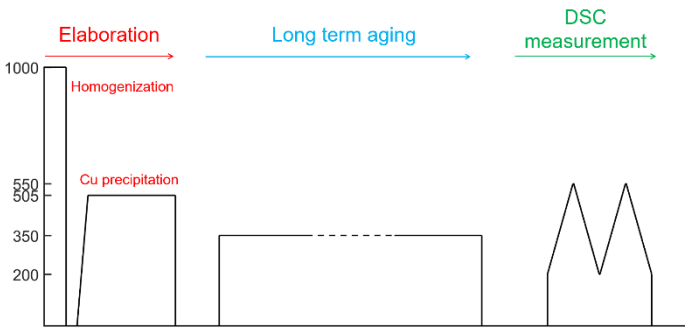

Figure 1: Schematic temperature evolution versus time of the DSC samples from elaboration of the alloy to the DSC experiment.

3. Results

Before the interpretation of the measured heat flow variation during temperature scanning, a correction of the data is needed to isolate the DSC signal originating from the reversion of the Fe-Cr unmixing only. Indeed, the material under study possesses a rather complex microstructure and possible other contributions – originating from other microstructural features – may be present in the measured data. We have to make sure that we only consider the signal contribution of the reversion of the Fe-Cr unmixing before processing the data. We will detail in the two following paragraph the two major complementary corrections we applied on the raw data.

Firstly, we draw attention to the fact that the solutionizing of the Fe and Cr composition fluctuations may be considered as a non-reversible solid state transformation – opposed to more conventional precipitates dissolution during heating and re-precipitation during cooling. Indeed, the solutionizing of the Fe and Cr composition fluctuations is rapid above their temperature of formation (400-600°C) whereas their formation (at 300-400°C) is very slow. Thus we can make the following hypothesis: the solutionizing during the heating ramp will be complete and no unmixing will occur during the cooling ramp.

To verify this hypothesis, we applied two consecutive scanning cycles to both unaged and aged specimens. These measurements showed that for the aged specimen an endothermic peak is observed during the first heating ramp, no corresponding exothermic peak is observed during the consecutive cooling ramp and no endothermic nor exothermic peaks are observed during the consecutive cycle whereas for the unaged specimen no evolution of the heat flux variation during scanning is observed between the first and the second thermic cycle (these measurements are shown in supplementary material). Moreover, the measurement obtained during the second thermal cycle for an aged specimen is similar to the ones obtained for an unaged specimen. Based on these observations, we conclude that the measurement obtained during a second heating ramp can be used as a baseline to correct the measurement obtained during the first heating ramp. We subtracted a straight line so the corrected heat flux is constant – equal to 0 – between 250 and 325°C, to eliminate a possible small deviation of the instrument baseline between the two consecutive heating ramps.

The second correction we applied to the DSC data concerns the high-temperature part of the solutionizing peak. For the most advanced stages of unmixing, the peak is spread beyond the maximum temperature of the measuring range (550°C, limitation of the instrument) and in the case of the very early stages of the unmixing corresponding to very weak signals the end

of the peak may be difficult to separate from other weak signals in the high-temperature range.

To overcome these two obstacles, we chose to model the peak shape and to use an extrapolated reconstruction of the high-temperature side of the peak for the calculation of the solutionizing enthalpy. Our methodology to do so was to use the experimental data only until 30°C above the peak temperature of the endothermic reaction, and to use extrapolated data above. To estimate the extrapolated data, the experimental data was fitted in the above-mentioned range with a pseudo-Voigt function, whose value was then used instead of the experimental data in the high-temperature range. An example of a complete set of the corrected data for one aging temperature – 325°C – is shown in **Figure 2**. The corrected measured data is displayed as solid lines and the reconstructed data based on the pseudo-Voigt fit is displayed as dotted lines.

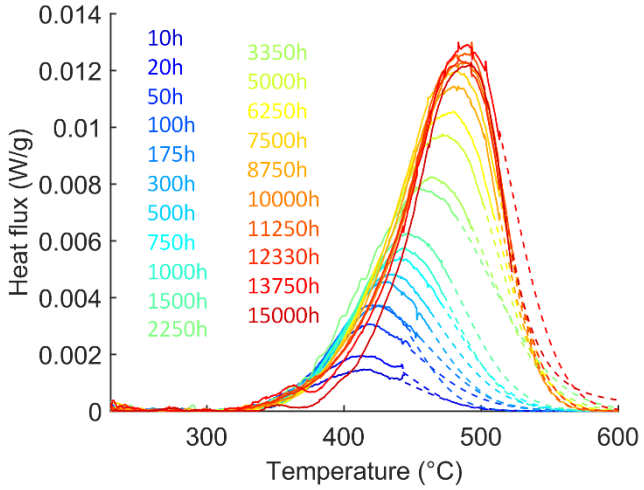

Figure 2: Complete set of corrected DSC data for the aging at 325°C. The measured data is displayed in solid lines and the corresponding fitted data (high temperature part of the peak) is displayed in dotted lines.

From the corrected data, we deduced two characteristics of the solutionizing of Fe and Cr composition fluctuations:

- The peak temperature. If we assume that in all cases the solutionizing of Fe-Cr unmixing is triggered at the same starting temperature, then at a constant heating rate the peak temperature represents the extent of diffusion which is needed to dissolve the Cr-rich regions and thus should be linked to the characteristic length of the Fe and Cr composition fluctuations.
- The solutionizing enthalpy – the integrated heat flux, named transformation enthalpy in the following – which is linked to the advancement of the unmixing reaction, and should be related to the amplitude of the composition fluctuations.

As can be observed on the DSC dataset for multiple aging durations at a single temperature in **Figure 2**, both these DSC characteristics increase with aging time. This evolution of both peak temperature and transformation enthalpy at all the studied aging temperatures is displayed in **Figure 3**.

Considering **Figure 2** and **Figure 3**, we may also point out that DSC is a very sensitive technique if we compare these measurements to previous studies [24,31]. Indeed, significant peak temperatures and transformation enthalpies are measured even for extremely short aging durations – down to 10 h – at low temperatures – 290°C and 325°C – and a significant increase of both these Fe-Cr unmixing quantifiers may be observed for very early stages.

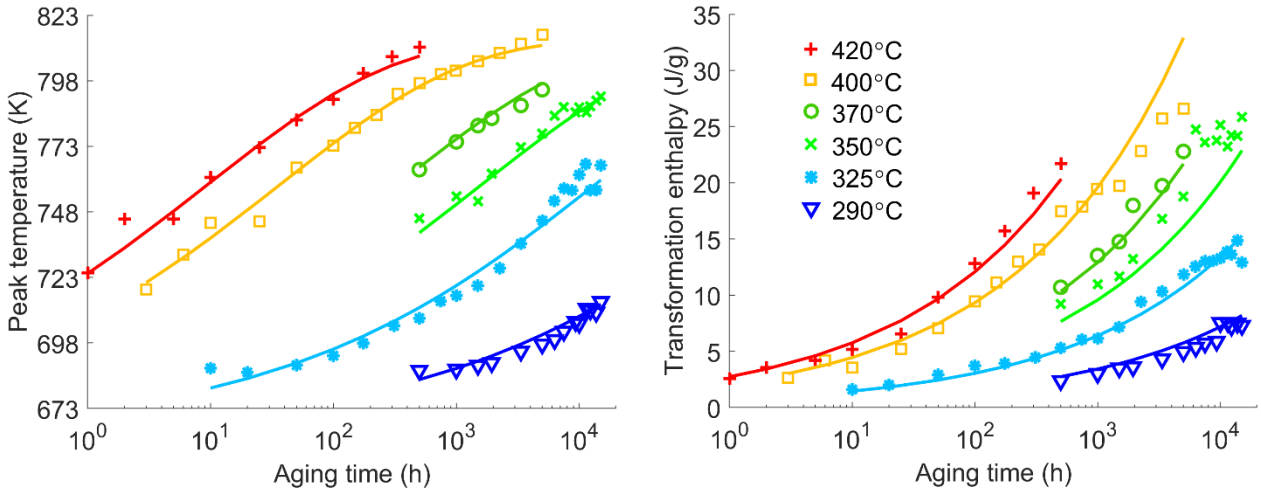

Figure 3: Kinetics of evolution of peak temperature and transformation enthalpy of the solutionizing of Fe and Cr composition fluctuautions obtained after aging for different durations at six different temperatures. Solid lines are guides for the eye.

4. Discussion

As previously mentioned, all the aging conditions characterised here using DSC have already been characterised using SAXS – the material used for both techniques extracted from the same aged samples for each aging condition. Several authors have characterised the Fe-Cr compositions fluctuations appearing and developing during unmixing in terms of amplitude and characteristic length using APT (based on 1D autocorrelation function and radial distribution functions or RDFs more recently) [2,9,11,13,25,29]. In addition, we already showed that the RDFs extracted from APT datasets and from SAS data can be analysed in a common framework leading to an equivalent characterisation of the Fe-Cr composition fluctuations in terms of amplitude and characteristic length [31].Thus, we will use our SAXS measurements as Fe-Cr composition fluctuations reference descriptors to compare with the characteristics obtained from the DSC temperature scans.

We describe the parameters extracted from DSC data by phenomenological models whereby the prefactor of the aging time power-law can be expressed using an Arrhenius equation. For the transformation enthalpy H, it reads:

$$H = \left(k_{0H}.exp\left(-\frac{Q_H}{RT}\right).t\right)^{a_H} \quad (1)$$

where k_{0H} and a_H are constants – 1.1x10^{13} $(\mathrm{J.g^{-1}})^{-a_H}.h^{-1}$ and 0.31 respectively –, Q_H is the Arrhenius function's activation energy – 155 kJ.mol^{-1} – and t and T are the aging duration and temperature respectively. For the peak temperature T_p the model has a different form due to the presence of asymptotic behavior for elevated temperatures:

$$T_p = T_{p_0} + \Delta T_p \left(1 - exp\left(-\left(k_{0T_p}.exp\left(-\frac{Q_{T_p}}{RT}\right).t\right)^{a_{T_p}}\right)\right) \quad (2)$$

where T_{p_0}, ΔT_p, k_{0T_p} and a_{T_p} are constants – 663 K, 151 K, 7.4x10^{18} h^{-1}. and 0.29 respectively –, Q_{T_p} is the Arrhenius function's activation energy – 263 kJ.mol^{-1} – and t and T are the aging duration and temperature respectively.

As we previously reported for the amplitude and correlation length [24], the activation energies associated with the transformation enthalpy and the peak temperature are significantly different. The one associated with the peak temperature is close to the activation energy of Cr diffusion in body-centered cubic iron (240 kJ.mol^{-1} [40–42]) which was also the case of the activation energy associated with the correlation length of Cr composition fluctuations (269 kJ.mol^{-1})[24]. This result is consistent with the hypothesis that the peak temperature measured in DSC for the Cr composition fluctuations solutionizing is controlled by the characteristic spatial extension of these fluctuations, hence the Cr atoms diffusion distance.

On the contrary, the value associated with the transformation enthalpy is significantly smaller than the Cr diffusion activation energy, close to that associated with the Cr composition

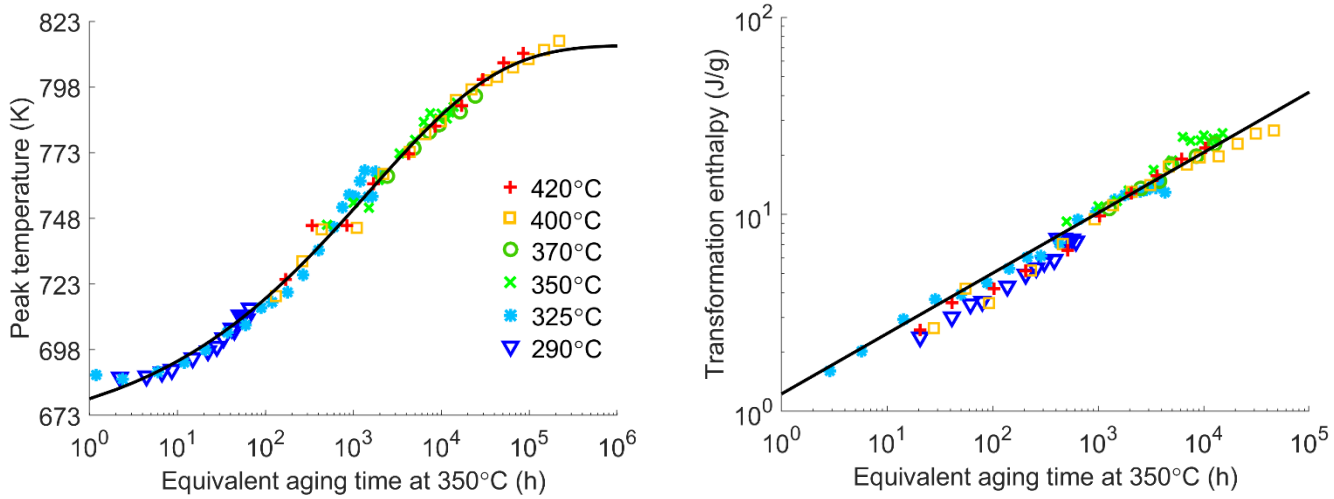

Figure 4: Equivalent aging time representation of the peak temperature (left hand side) and the transformation enthalpy (right hand side) for all aging conditions. The solid line in each graph is the master curve fitted to all data points.

fluctuations' amplitude – 126 kJ.mol^{-1} [24]. Again, this result is consistent with the hypothesis that the transformation enthalpy is linked to the Fe-Cr unmixing advancement and not to the Cr atoms characteristic diffusion length during solutionizing.

Now that we determined the activation energies associated with both peak temperature and transformation enthalpy evolution during aging, we can use an equivalent aging temperature description to represent the DSC data measured at the six aging temperatures for a single arbitrary chosen aging temperature – here 350°C, being the most relevant for the material application. This equivalent aging temperature representation is based on the existence of a single activation energy associated with the unmixing quantifiers' evolution over the whole aging temperature range considered. It is introduced in details in our previous work [24]. On this simplified representation given in **Figure 4**, we can observe that all data points gather on

a single master curve that can be modeled using equations (1) and (2) at the equivalent aging temperature.

As we mentioned, the activation energies associated with the correlation length of Cr composition fluctuations (SAXS) and with the peak temperature (DSC) on one hand and with the amplitude of Cr composition fluctuations (SAXS) and the transformation enthalpy (DSC) on the other hand are quite close from each other. This observation may indicate a correlation between the Fe-Cr unmixing quantifiers measured using SAXS and DSC. The relationships existing between them are illustrated in **Figure 5** by plotting the SAXS correlation length versus the DSC peak temperature (graph on the left-hand side) and the SAXS amplitude versus the DSC transformation enthalpy (graph on the right-hand side). These graphs show phenomenological relationships between the unmixing quantifiers obtained with DSC and the physical descriptors obtained with SAS. The relationships presented in this work between the SAXS and DSC characterizations allow the determination of Cr composition fluctuation's amplitude and correlation length knowing the transformation enthalpy and the peak temperature respectively.

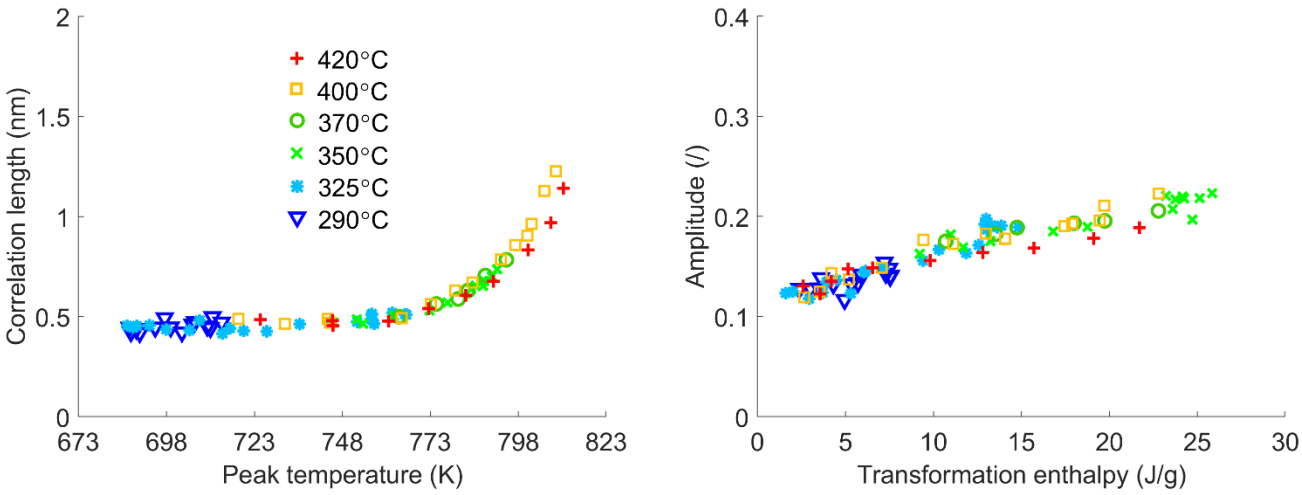

Figure 5: Comparison between the SAXS and DSC quantifiers. On the left hand side, correlation length of the Cr composition fluctuations measured in SAXS versus the peak temperature obtained in DSC. On the right hand side, amplitude of the Cr composition fluctuations measured in SAXS versus the transformation enthalpy obtained in DSC.

5. Conclusions

This work shows that the Fe-Cr unmixing characterization in stainless steels, which normally involves advanced instrumentation such as synchrotrons, neutrons or APT, can be as accurately performed using DSC with a quite easy to implement methodology consisting of two successive temperature scans up to 550°C. The subtraction of the two scans leads to the measurement of the transformation enthalpy and the peak temperature of the endothermic peak corresponding to the Fe and Cr atoms solutionizing. The first parameter is related to the advancement of the unmixing reaction and the second one is related to the characteristic size of the unmixing.

By comparing the characterization of the Cr composition fluctuation occurring during aging obtained by SAXS and DSC, we showed that these two are directly correlated. The phenomenological relationships presented in this work can be used to access the physical

descriptors of the Cr composition fluctuations – its amplitude and characteristic length – using a DSC experiment which is much easier to implement compared to a synchrotron SAXS experiment. This may allow studies of the Fe-Cr unmixing including numerous aging conditions and/or the use of this technique to follow the long term ageing of stainless steel components during use in the industry.

Acknowledgments

Dr. J. Hugues of CIRIMAT laboratory is thanked for realizing some of the aging heat treatments of this study. The technical staff of ESRF-D2AM beamline is thanked for technical help during the SAXS experiments. Janine Sziklasi is thanked for her help in the preparation and realization of a large part of the numerous DSC experiments.

Declarations of interest: none

Funding: This work was supported by the Agence Nationale de la Recherche (ANR, France) [grant number ANR-10-RMNP-0017]

References

[1] P.J. Grobner, The 885° f (475° c) embrittlement of ferritic stainless steels, Metall. Trans. 4 (1973) 251–260. https://doi.org/10.1007/BF02649625.

[2] F. Danoix, P. Auger, Atom Probe Studies of the Fe–Cr System and Stainless Steels Aged at Intermediate Temperature: A Review, Mater. Charact. 44 (2000) 177–201. https://doi.org/10.1016/S1044-5803(99)00048-0.

[3] J.K. Sahu, U. Krupp, R.N. Ghosh, H.-J. Christ, Effect of 475 °C embrittlement on the mechanical properties of duplex stainless steel, Mater. Sci. Eng. A. 508 (2009) 1–14. https://doi.org/10.1016/j.msea.2009.01.039.

[4] P. Hedström, F. Huyan, J. Zhou, S. Wessman, M. Thuvander, J. Odqvist, The 475°C embrittlement in Fe–20Cr and Fe–20Cr–X (X=Ni, Cu, Mn) alloys studied by mechanical testing and atom probe tomography, Mater. Sci. Eng. A. 574 (2013) 123–129. https://doi.org/10.1016/j.msea.2013.03.016.

[5] A. Takahashi, T. Suzuki, A. Nomoto, T. Kumagai, Influence of spinodal decomposition structures on the strength of Fe-Cr alloys: A dislocation dynamics study, Acta Mater. 146 (2018) 160–170. https://doi.org/10.1016/j.actamat.2017.12.051.

[6] M.K. Miller, J. Bentley, APFIM and AEM investigation of CF8 and CF8M primary coolant pipe steels, Mater. Sci. Technol. 6 (1990) 285–292. https://doi.org/10.1179/mst.1990.6.3.285.

[7] J.E. Brown, G.D.W. Smith, Atom probe studies of spinodal processes in duplex stainless steels and single- and dual-phase Fe-Cr-Ni alloys, Surf. Sci. 246 (1991) 285–291. https://doi.org/10.1016/0039-6028(91)90428-U.

[8] F. Danoix, P. Auger, D. Blavette, An atom-probe investigation of some correlated phase transformations in Cr, Ni, Mo containing supersaturated ferrites, Surf. Sci. 266 (1992) 364–369. https://doi.org/10.1016/0039-6028(92)91047-F.

[9] J.M. Hyde, A. Cerezo, M.K. Miller, G.D.W. Smith, A critical comparison between experimental results and numerical simulations of phase separation in the Fe-Cr system, Appl. Surf. Sci. 76–77 (1994) 233–241. https://doi.org/10.1016/0169-4332(94)90348-4.
[10] M. Murayama, K. Hono, Y. Katayama, Microstructural evolution in a 17-4 PH stainless steel after aging at 400°C, Metall. Mater. Trans. A. 30 (1999) 345–353. https://doi.org/10.1007/s11661-999-0323-2.
[11] J. Zhou, J. Odqvist, M. Thuvander, P. Hedström, Quantitative Evaluation of Spinodal Decomposition in Fe-Cr by Atom Probe Tomography and Radial Distribution Function Analysis, Microsc. Microanal. 19 (2013) 665–675. https://doi.org/10.1017/S1431927613000470.
[12] J. Zhou, J. Odqvist, L. Höglund, M. Thuvander, T. Barkar, P. Hedström, Initial clustering – a key factor for phase separation kinetics in Fe–Cr-based alloys, Scr. Mater. 75 (2014) 62–65. https://doi.org/10.1016/j.scriptamat.2013.11.020.
[13] C. Pareige, J. Emo, S. Saillet, C. Domain, P. Pareige, Kinetics of G-phase precipitation and spinodal decomposition in very long aged ferrite of a Mo-free duplex stainless steel, J. Nucl. Mater. 465 (2015) 383–389. https://doi.org/10.1016/j.jnucmat.2015.06.017.
[14] T.G. Lach, A. Devaraj, K.J. Leonard, T.S. Byun, Co-dependent microstructural evolution pathways in metastable δ-ferrite in cast austenitic stainless steels during thermal aging, J. Nucl. Mater. 510 (2018) 382–395. https://doi.org/10.1016/j.jnucmat.2018.08.038.
[15] R. Badyka, G. Monnet, S. Saillet, C. Domain, C. Pareige, Quantification of hardening contribution of G-Phase precipitation and spinodal decomposition in aged duplex stainless steel: APT analysis and micro-hardness measurements, J. Nucl. Mater. 514 (2019) 266–275. https://doi.org/10.1016/j.jnucmat.2018.12.002.
[16] J.C. LaSalle, L.H. Schwartz, Further studies of spinodal decomposition in Fe-Cr, Acta Metall. 34 (1986) 989–1000. https://doi.org/10.1016/0001-6160(86)90208-7.
[17] M. Furusaka, Y. Ishikawa, S. Yamaguchi, Y. Fujino, Phase Separation Process in FeCr Alloys Studied by Neutron Small Angle Scattering, J. Phys. Soc. Jpn. 55 (1986) 2253–2269. https://doi.org/10.1143/JPSJ.55.2253.
[18] J.P. Simon, O. Lyon, Phase separation in a Fe-Cr-Co alloy studied by anomalous small angle X-ray scattering, Acta Metall. 37 (1989) 1727–1733. https://doi.org/10.1016/0001-6160(89)90058-8.
[19] F. Bley, Neutron small-angle scattering study of unmixing in Fe-Cr alloys, Acta Metall. Mater. 40 (1992) 1505–1517. https://doi.org/10.1016/0956-7151(92)90094-U.
[20] C.H. Shek, Y.Z. Shao, K.W. Wong, J.K.L. Lai, Spatial fractal characteristic of spinodal decomposition in Fe-Cr-Ni duplex stainless steel, Scr. Mater. 37 (1997) 529–533. https://doi.org/10.1016/S1359-6462(97)00136-X.
[21] T. Ujihara, K. Osamura, Kinetic analysis of spinodal decomposition process in Fe–Cr alloys by small angle neutron scattering, Acta Mater. 48 (2000) 1629–1637. https://doi.org/10.1016/S1359-6454(99)00441-3.
[22] M. Hörnqvist, M. Thuvander, A. Steuwer, S. King, J. Odqvist, P. Hedström, Early stages of spinodal decomposition in Fe–Cr resolved by in-situ small-angle neutron scattering, Appl. Phys. Lett. 106 (2015) 061911. https://doi.org/10.1063/1.4908250.
[23] O. Tissot, C. Pareige, M.-H. Mathon, M. Roussel, E. Meslin, B. Décamps, J. Henry, Comparison between SANS and APT measurements in a thermally aged Fe-19 at.%Cr alloy, Mater. Charact. 151 (2019) 332–341. https://doi.org/10.1016/j.matchar.2019.03.027.

[24] L. Couturier, F. De Geuser, A. Deschamps, Microstructural evolution during long time aging of 15–5PH stainless steel, Materialia. 9 (2020) 100634. https://doi.org/10.1016/j.mtla.2020.100634.
[25] Y. Das, J. Liu, S. Wessman, X. Xu, J. Odqvist, S. King, P. Hedström, Small-angle neutron scattering quantification of phase separation and the corresponding embrittlement of a super duplex stainless steel after long-term aging at 300°C, Materialia. (2020) 100771. https://doi.org/10.1016/j.mtla.2020.100771.
[26] J.M. Hyde, M.K. Miller, M.G. Hetherington, A. Cerezo, G.D.W. Smith, C.M. Elliott, Spinodal decomposition in Fe-Cr alloys: Experimental study at the atomic level and comparison with computer models—II. Development of domain size and composition amplitude, Acta Metall. Mater. 43 (1995) 3403–3413. https://doi.org/10.1016/0956-7151(95)00041-S.
[27] F. Danoix, P. Auger, D. Blavette, Hardening of Aged Duplex Stainless Steels by Spinodal Decomposition, Microsc. Microanal. 10 (2004) 349–354.
[28] C. Pareige, S. Novy, S. Saillet, P. Pareige, Study of phase transformation and mechanical properties evolution of duplex stainless steels after long term thermal ageing (>20 years), J. Nucl. Mater. 411 (2011) 90–96. https://doi.org/10.1016/j.jnucmat.2011.01.036.
[29] J. Emo, C. Pareige, S. Saillet, C. Domain, P. Pareige, Kinetics of secondary phase precipitation during spinodal decomposition in duplex stainless steels: A kinetic Monte Carlo model – Comparison with atom probe tomography experiments, J. Nucl. Mater. 451 (2014) 361–365. https://doi.org/10.1016/j.jnucmat.2014.04.025.
[30] N. Pettersson, S. Wessman, M. Thuvander, P. Hedström, J. Odqvist, R.F.A. Pettersson, S. Hertzman, Nanostructure evolution and mechanical property changes during aging of a super duplex stainless steel at 300°C, Mater. Sci. Eng. A. 647 (2015) 241–248. https://doi.org/10.1016/j.msea.2015.09.009.
[31] L. Couturier, F. De Geuser, A. Deschamps, Direct comparison of Fe-Cr unmixing characterization by atom probe tomography and small angle scattering, Mater. Charact. 121 (2016) 61–67. https://doi.org/10.1016/j.matchar.2016.09.028.
[32] F. De Geuser, B. Gault, Metrology of small particles and solute clusters by atom probe tomography, Acta Mater. 188 (2020) 406–415. https://doi.org/10.1016/j.actamat.2020.02.023.
[33] E. Herny, E. Andrieu, J. Lacaze, F. Danoix, N. Lecoq, Study by Differential Thermal Analysis of Reverse Spinodal Transformation in 15-5 PH Alloy., Solid State Phenom. 172–174 (2011) 338–343. https://doi.org/10.4028/www.scientific.net/SSP.172-174.338.
[34] C. Capdevila, M.K. Miller, F.A. López, G. Pimentel, J. Chao, Reverse α–α′ phase separation in Fe-20Cr-6Al alloy, Philos. Mag. 93 (2013) 1640–1651. https://doi.org/10.1080/14786435.2012.750768.
[35] L. Couturier, F. De Geuser, M. Descoins, A. Deschamps, Evolution of the microstructure of a 15-5PH martensitic stainless steel during precipitation hardening heat treatment, Mater. Des. 107 (2016) 416–425. https://doi.org/10.1016/j.matdes.2016.06.068.
[36] F. Zhang, J. Ilavsky, G.G. Long, J.P.G. Quintana, A.J. Allen, P.R. Jemian, Glassy Carbon as an Absolute Intensity Calibration Standard for Small-Angle Scattering, Metall. Mater. Trans. A. 41 (2010) 1151–1158. https://doi.org/10.1007/s11661-009-9950-x.
[37] K.J. Jones, I. Kinshott, M. Reading, A.A. Lacey, C. Nikolopoulos, H.M. Pollock, The origin and interpretation of the signals of MTDSC, Thermochim. Acta. 304–305 (1997) 187–199. https://doi.org/10.1016/S0040-6031(97)00096-8.

[38] E. Verdonck, K. Schaap, L.C. Thomas, A discussion of the principles and applications of Modulated Temperature DSC (MTDSC), Int. J. Pharm. 192 (1999) 3–20. https://doi.org/10.1016/S0378-5173(99)00267-7.
[39] Z. Jiang, C.T. Imrie, J.M. Hutchinson, An introduction to temperature modulated differential scanning calorimetry (TMDSC): a relatively non-mathematical approach, Thermochim. Acta. 387 (2002) 75–93. https://doi.org/10.1016/S0040-6031(01)00829-2.
[40] A.W. Bowen, G.M. Leak, Diffusion in Bcc iron base alloys, Metall. Trans. 1 (1970) 2767–2773. https://doi.org/10.1007/BF03037813.
[41] R.A. Wolfe, H.W. Paxton, DIFFUSION IN B.C.C. METALS, CARNEGIE INST OF TECH PITTSBURGH PA, 1964. https://apps.dtic.mil/docs/citations/AD0434751.
[42] A.-M. Huntz, M. Aucouturier, P. Lacombe, Mesure des coefficients de diffusion en volume et intergranulaire du chrome radioactif dans le fer alpha, Comptes Rendus Académie Sci. 265 (1967) 554–557.

Supplementary materials

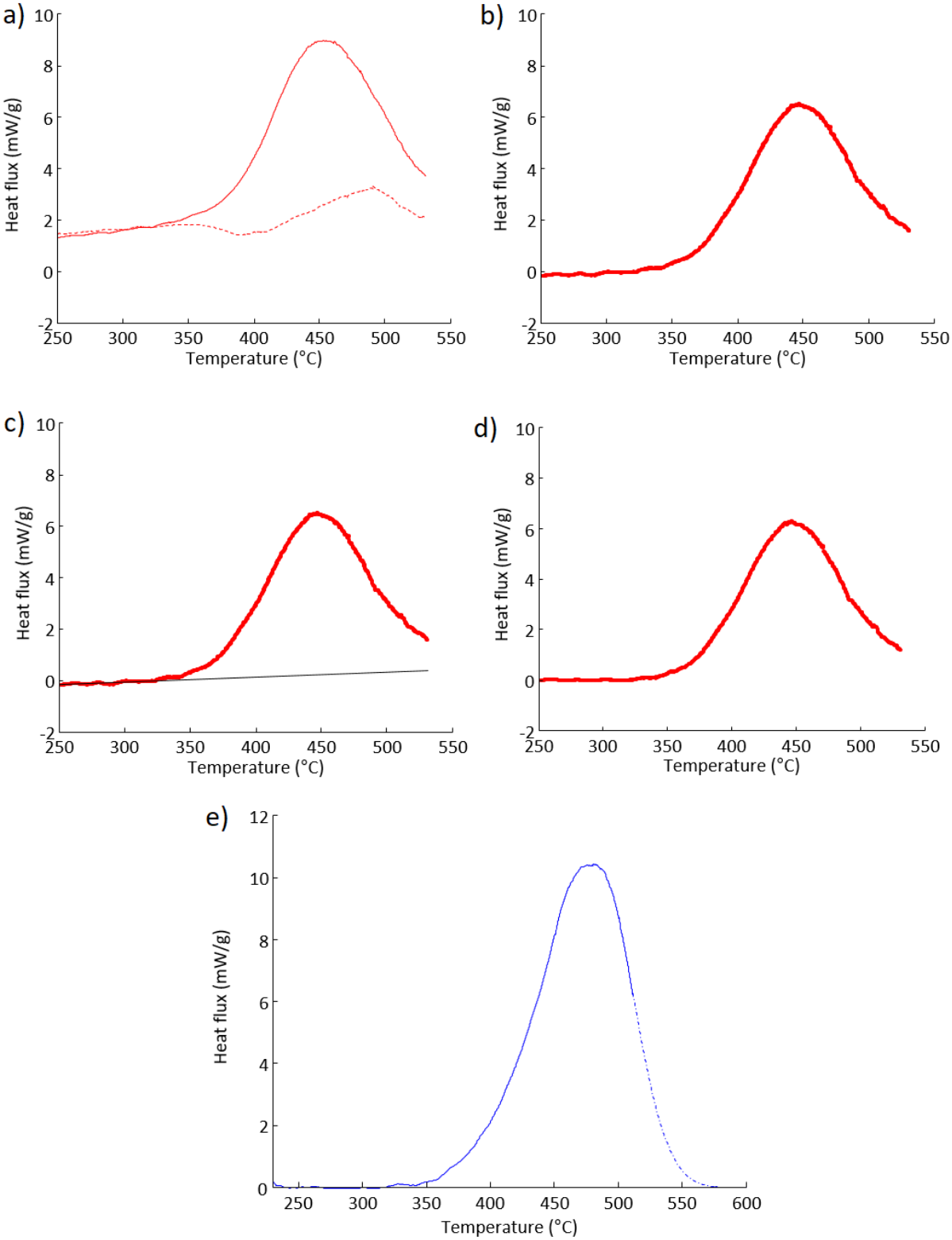

Figure 6: Graph a) represents the heat flow evolution acquired on an aged sample during a first heating scan (solid line) together with the one acquired during a subsequent heating scan (dotted line) which can be used as a baseline. Graph b) is the result of the subtraction of this baseline from the first heating scan. Graph c) illustrates the slight linear deviation remaining in the subtracted heat flow (black straight line). Graph d) is the result of the subtraction of this slight linear deviation from the subtracted heat flow. Finally graph e) represents this corrected heat flow. In this graph the experimental data are cut off above the temperature of the peak maximum plus 30°C (solid line) the rest (dotted line) is steaming from the fit of the peak with a pseudo-Voigt function.